弾塑性地盤力学に基づく一様圧縮作用下でのImbricationおよびデコルマの形成解析

Formation simulation of imbrication and décollement under uniform compression based on the elasto-plastic soil mechanics

*豊田 智大[1]、野田 利弘[1]、大西 和也[2]、浅岡 顕[3]
*Tomohiro Toyoda[1], Toshihiro Noda[1], Kazuya Onishi[2], Akira Asaoka[3]

1. 名古屋大学　減災連携研究センター、2. 名古屋大学　工学部、3. 地震予知総合研究振興会
1. Nagoya University, Disaster Mitigation Research Center, 2. Nagoya University, School of Engineering, 3. Association for the Development of Earthquake Prediction

水平圧縮を受ける地盤においては，構成材料や境界条件に応じて，多種多様な地形が生じることが知られている．地盤内での単一の変位不連続に限定しても，発生角度が45°以上の「逆断層」，45°未満の「衝上断層」，水平に滑動する「デコルマ」が存在する．さらに，これらのすべり線が複数生じて地盤のpartitioningが進むと，共役なすべりに挟まれたブロックが隆起する「pop-up」や，平行な衝上断層群である「imbrication」など，さまざまな断層変位地形が形成されてゆく．このような地形の非可逆的かつ多段階に亘る形成過程を数値解析により解くためには，(1)地盤材料の材料非線形性，とくに軟化現象を表現可能な弾塑性構成式，および(2)地盤の形状および状態の変化を刻々と追跡可能な有限変形理論に基づいて解析を行う必要がある．本報では，端緒的ではあるが，著者らが開発した(1)(2)の点および間隙水の存在と慣性力を考慮可能な地盤の変形解析コード***GEOASIA***[1]により，上に挙げた種々の圧縮地形の形成解析を行った結果を紹介する．

まず，境界条件の異なる図-1(a)-(c)の3種類の二次元平面ひずみ有限要素メッシュを用意して弾塑性変形解析を行った．構成材料は間隙水の存在を考慮しない一相系弾塑性体とし，物体力として自重を考慮した．弾塑性構成式には，土の骨格構造を記述可能なSYS Cam-clay model[2]を用いた．材料定数および初期状態はNoda et al.[3]に準拠した．その詳細は紙幅の都合上割愛するが，材料を「超過圧密土」とすることで，ピーク強度発現後の顕著な軟化挙動（図-2）を示すようパラメータを設定した．代表的な時点におけるせん断ひずみ分布を図-3に示す．模型底面において，応力境界（せん断応力ゼロ）を設定した同図(a)では「pop-up」が解かれたのに対し，変位速度境界（一様圧縮）を与えた(b)では「imbrication」が解かれることを示した．さらに，(b)の解析結果を右端の側面摩擦を外した(c)と比較すると，Imbricationの発生間隔が異なるのみならず，衝上順序についても，(b)では最初のすべりの下盤側にすべりが形成されてゆく「piggyback型」となるのに対し，(b)では上盤側にすべりが形成されてゆく「overstep型」となった．このように，非可逆的かつ多段階に亘る圧縮場における局所化の進展を弾塑性有限変形解析により再現するとともに，その様相が境界条件に応じて大きく異なることを示した．図-1で与えた境界条件はいずれも非常に単純なものばかりであるにもかかわらず，これだけ多様な変形が解かれる点は非常に興味深い．なお，すべりの発生角度はいずれも限界状態定数より予測されるMohr-Coulombのすべり角に一致することを確認している．

次に，間隙水で満たされた飽和地盤を想定して二相系（水～土骨格連成）弾塑性解析を実施した．有限要素メッシュおよび境界条件は図-1(c)と同一のものを用いるとともに，材料定数はYamada et al.[4]に準拠し，続成作用により半固結状態にある地盤を想定して，初期過圧密比と同程度の初期構造を与えた．このとき，材料の挙動は拘束圧のみならず排水距離によっても変化し，幅1要素の解析においては，深度に応じて同図(b)のような軟化挙動を示す．解析により得られたせん断ひずみ分布の推移を図-5に示す．解析初期においては同図(a)のようなImbricationの予兆が確認されるが，更に変形が進行した(b)では模型中央深さにおいて水平すべり（デコルマ）の発生が解かれ，その後(c)(d)では，最初のデコルマの下盤側で2本目のすべりを生じ，領域Iの底に領域IIが付加される様子が解かれた．変形の過程では，材料のダイレイタンシー（塑性圧縮）に起因する正の過剰間隙水圧の発生（図-6）や，脆性的な変形の局所化に伴う地震動の発生（図-7）が解かれた．今後は，部分排水の程度の影響や寸法効果についても検討してゆきたい．

（謝辞）本研究の実施にあたり，科学研究費補助金（基盤研究(A)：課題番号17H01289）の助成を受けた．

[1] Asaoka, A., Noda, T., Yamada, E., Kaneda, K. and Nakano, M. (2002): An Elasto-plastic description of

two distinct volume change mechanisms of soils, Soils and Foundations, Vol.42, No.5, pp.47-57.

[2] Noda, T., Asaoka, A. and Nakano, M. (2008): Soil-water coupled finite deformation analysis based on a rate-type equation of motion incorporating the SYS Cam-clay model, Soils and Foundations, Vol.48, No.6, pp.771-790.

[3] 野田利弘, 山田正太郎, 豊田智大, 浅岡顕 (2015): 横ずれ断層に伴う表層地盤のリーデルせん断帯の形成に及ぼす材料的初期不整の影響, 土木学会論文集A2, Vol.71, No.2, I_463-I_474.

[4] Yamada, E., Nakai, K. and Asaoka, A. (2021): Soil-water coupled elasto-plastic analysis on the formation process of normal faults in submarine ground due to its uplift and inclination, Proc. 20th Int. Conf. on Soil Mechanics and Geotechnical Engineering (Accepted).

キーワード：圧縮、衝上断層、覆瓦状構造、デコルマ、弾塑性、有限要素解析
Keywords: Compression, Thrust fault, Imbrication, Décollement, Elasto-plasticity, Finite element analysis

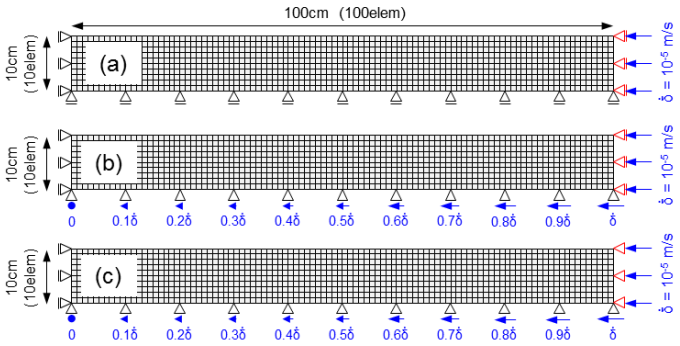

Figure 1. Finite element mesh

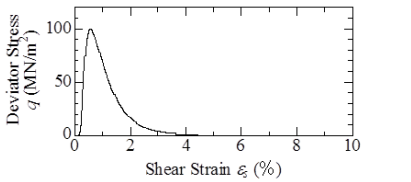

Figure 2. Drained triaxial compression behavior (p_0' = 82.8kPa)

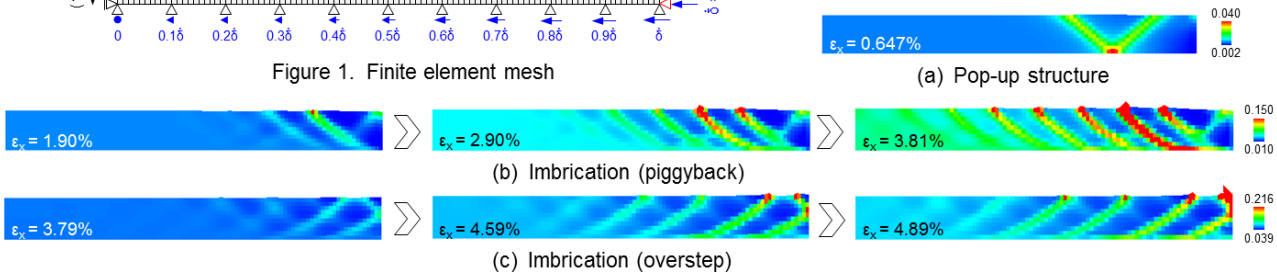

Figure 3. Shear strain distribution (single-phase analysis) (ε_x : horizontal strain of the model)

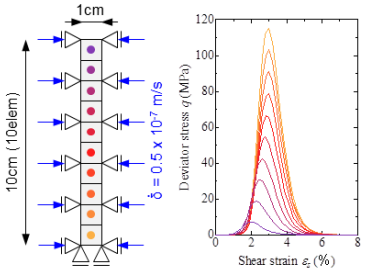

Figure 4. Lateral compressive behavior of one-element width analysis (plane-strain condition)

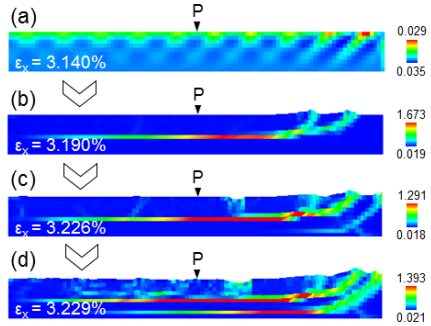

Figure 5. Shear strain distribution (two-phase analysis)

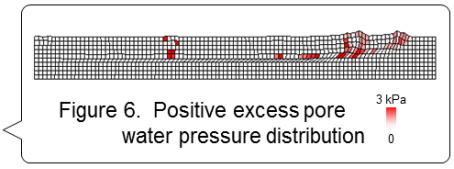

Figure 6. Positive excess pore water pressure distribution

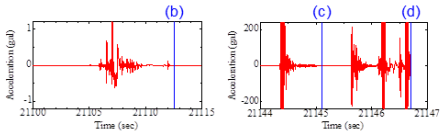

Figure 7. Vertical acceleration at point P in Fig. 5

Formation simulation of imbrication and décollement under uniform compression based on the elasto-plastic soil mechanics

*Tomohiro Toyoda[1], Toshihiro Noda[1], Kazuya Onishi[2], Akira Asaoka[3]

1. Nagoya University, Disaster Mitigation Research Center, 2. Nagoya University, School of Engineering, 3. Association for the Development of Earthquake Prediction

A wide variety of topography is known to be formed in the ground subjected to lateral compression, depending on the constituent materials and boundary conditions. In terms of a single displacement discontinuity, there exist "reverse faults" over 45 degree, “thrust faults” under 45 degree, and horizontal "décollements". A partitioned ground by the faults exhibits a “pop-up” structure with conjugate slip surfaces or “imbrication” with parallel slip surfaces. To simulate their irreversible and multi-step formation process, (1) the elasto-plastic constitutive model for describing material nonlinearity and (2) finite deformation scheme for tracing changes in shape and state of the ground are necessary. In this abstract, we introduce the results of the formation analysis of these structures based on our analysis code *GEOASIA* [1] that can consider (1), (2), the presence of pore water, and dynamics.

First, an elasto-plastic deformation analysis was performed with three plane-strain finite element meshes with different boundary conditions shown in Fig. 1 (a)-(c). Here, we conducted a single-phase elasto-plastic analysis considering the self-weight of the model. SYS Cam-clay model [2] was incorporated as an elasto-plastic constitutive model. The overconsolidated parameters in Noda et al. [3] exhibiting remarkable softening behavior after the peak strength (Fig. 2) were used. The shear strain distributions in Fig. 3 indicate that the analysis without fixation of the bottom displacement in (a) exhibited pop-up, whereas the analysis with the prescription of the linear bottom displacement distribution (uniform compression) in (b) obtained imbrication. Furthermore, the separation of the imbrication and the thrust sequence, i.e., piggyback in (b) and overstep in (c), were affected by the presence of the end friction. We successfully simulated characteristic structures with the irreversible and multi-step strain localization in the compressed ground based on the elasto-plastic finite deformation analysis and confirmed the effect of boundary condition.

Next, the soil-water coupled elasto-plastic analysis for the saturated ground was conducted. Material constants of semi-consolidated ground were adopted conforming to Yamada et al. [4] and the identical mesh of Fig. 1(c) was used. The lateral compressive behavior obtained by analysis of one-element width is indicated in Fig. 4. Figure 5 shows the transition of the shear strain distribution. At the beginning of the analysis, the appearance of the imbrication was confirmed in (a). However, in (b), the occurrence of dé collement with horizontal slip was solved at the central depth of the model. Then, a second slip occurred on the lower side of the first décollement and the region II accreted to the bottom of the region I in (c)-(d). The occurrence of the positive excess pore water pressure (Fig. 6) and the generation of a seismic wave due to brittle deformation (Fig. 7) were also solved.

(Acknowledgement) We received Grant-in-Aid for Scientific Research (Grant-in-Aid for Scientific Research (A): No. 17H01289).

[1] Asaoka, A., Noda, T., Yamada, E., Kaneda, K. and Nakano, M. (2002): An elasto-plastic description of two distinct volume change mechanisms of soils, Soils and Foundations, Vol.42, No.5, pp.47-57.

[2] Noda, T., Asaoka, A. and Nakano, M. (2008): Soil-water coupled finite deformation analysis based on a rate-type equation of motion incorporating the SYS Cam-clay model, Soils and Foundations, Vol.48, No.6, pp.771-790.

[3] Noda, T., Yamada, S., Toyoda, T. and Asaoka, A. (2015): Effects of initial imperfection on the Riedel shear bands in surface ground due to strike-slip fault (in Japanese), Proc. of JSCE, Vol.71, No.2,

I_463-I_474.
[4] Yamada, E., Nakai, K. and Asaoka, A. (2021): Soil-water coupled elasto-plastic analysis on the formation process of normal faults in submarine ground due to its uplift and inclination, Proc. 20th Int. Conf. on Soil Mechanics and Geotechnical Engineering (Accepted).

Keywords: Compression, Thrust fault, Imbrication, Décollement, Elasto-plasticity, Finite element analysis

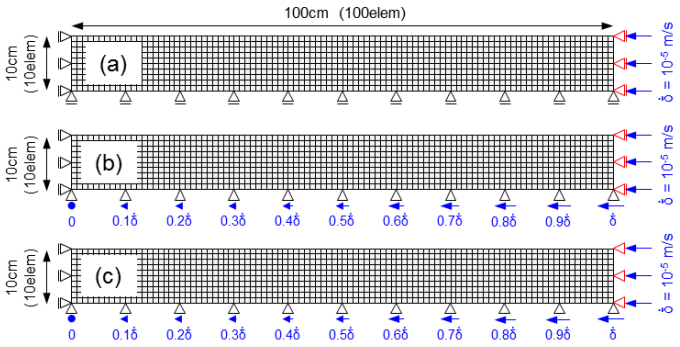

Figure 1. Finite element mesh

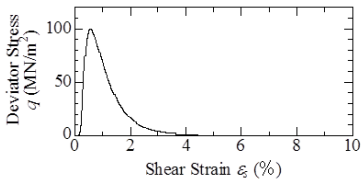

Figure 2. Drained triaxial compression behavior (p_0' = 82.8kPa)

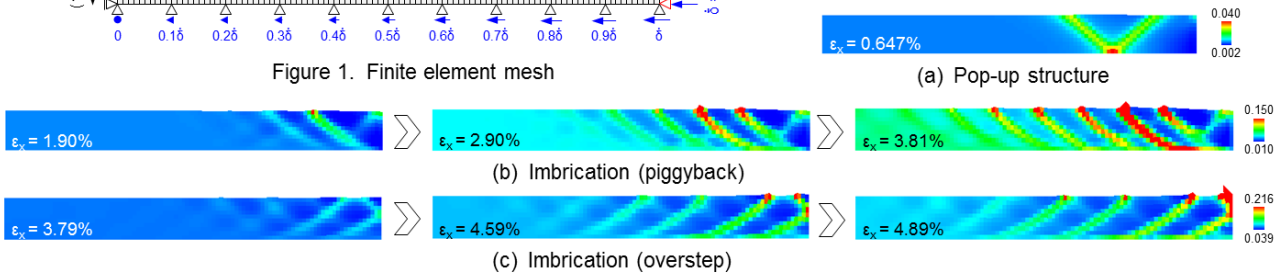

Figure 3. Shear strain distribution (single-phase analysis) (ε_x : horizontal strain of the model)

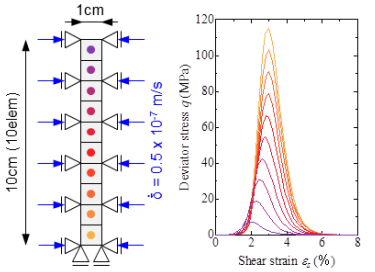

Figure 4. Lateral compressive behavior of one-element width analysis (plane-strain condition)

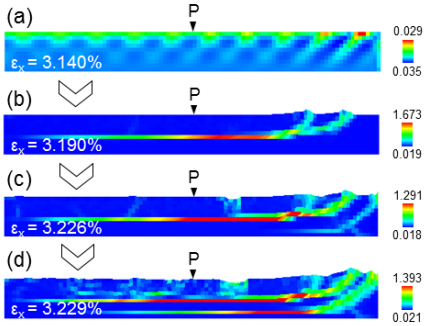

Figure 5. Shear strain distribution (two-phase analysis)

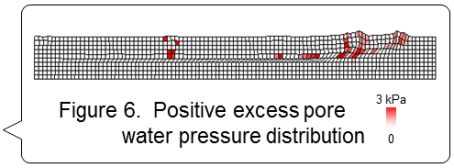

Figure 6. Positive excess pore water pressure distribution

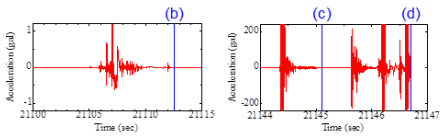

Figure 7. Vertical acceleration at point P in Fig. 5